

This is an electronic reprint of the original article. This reprint may differ from the original in pagination and typographic detail.

Preparation of three-dimensional cellulose objects previously swollen in a DMAc/LiCl solvent system

Obradovic, Jasmina; Wondraczek, Holger; Fardim, Pedro; Lassila, Lippo; Navard, Patrick

Published in:
Cellulose

DOI:
[10.1007/s10570-014-0403-3](https://doi.org/10.1007/s10570-014-0403-3)

Published: 01/01/2014

[Link to publication](#)

Please cite the original version:

Obradovic, J., Wondraczek, H., Fardim, P., Lassila, L., & Navard, P. (2014). Preparation of three-dimensional cellulose objects previously swollen in a DMAc/LiCl solvent system. *Cellulose*, 21(6), 4029–4038.
<https://doi.org/10.1007/s10570-014-0403-3>

General rights

Copyright and moral rights for the publications made accessible in the public portal are retained by the authors and/or other copyright owners and it is a condition of accessing publications that users recognise and abide by the legal requirements associated with these rights.

Take down policy

If you believe that this document breaches copyright please contact us providing details, and we will remove access to the work immediately and investigate your claim.

1

2 Preparation of three-dimensional cellulose 3 objects previously swollen in DMAc/LiCl 4 solvent system

5 Jasmina Obradovic¹ • Holger Wondraczek¹ • Pedro Fardim¹ • Lippo Lassila² •
6 Patrick Navard³

7

8 ¹Laboratory of Fibre and Cellulose Technology, Åbo Akademi, Porthansgatan 3, Turku, Finland

9 ²Department of Prosthetic Dentistry and Biomaterials Science, University of Turku,
10 Lemminkäisenkatu 2, FI-20520 Turku, Finland

11 ³Mines ParisTech, CEMEF – Centre de Mise en Forme des Matériaux, CNRS UMR 7635, BP 207,
12 1 rue Claude Daunesse, 06904 Sophia Antipolis Cedex, France

13 Author for correspondence (e-mail: pfardim@abo.fi; phone: +358-2-215-4126)

14

15

16 *Keywords: cellulose, compression moulding, pressure, N,N-dimethylacetamide,*
17 *swelling, mechanical properties*

18

19 Abstract

20

21 Three-dimensional shaped cellulosic objects were produced via a two-step
22 procedure: swelling of softwood pulp (93% cellulose; 4.5% hemicellulose; 54%
23 crystallinity) in DMAc/LiCl followed by moulding. Swollen cellulose pulp in the
24 form of gel was solidified with two different anti-solvents: distilled water and,
25 combination of 2-propanol and deionized water. The solid cellulose material was
26 further moulded in a custom-built prototype mould. Role of anti-solvent was to
27 solidify the swollen cellulose fibres and prepare mouldable solid specimens. The
28 anti-solvent was chosen based on the following criteria viz., recoverability, stable
29 chemical reactivity, availability, cost and previous research in the anti-solvent
30 area. The choice of solidification solvent had a great influence on the structure
31 and mechanical properties of the final cellulose material. Results of different
32 characterization techniques showed that when the cellulose gel was washed with
33 distilled water, it had a significantly higher amount of Lithium cations (ICP-MS
34 and Raman), amorphous structure (X-ray) and lower mechanical properties
35 (Nanoindentation), compared to samples washed with a combination of 2-
36 propanol and deionized water. Increase in viscosity as previously reported and
37 changes in the NMR and IR spectra of DMAc upon LiCl suggested the formation
38 of an ion-dipole complex, where Lithium cation resides adjacent to the oxygen of
39 the carbonyl group of DMAc. Formed macrocation [DMAc_n+Li]⁺ was preserved
40 between cellulose chains in cellulose specimens washed with distilled water and
41 had essential role in the disruption of initial bonds and thus enhancing
42 mouldability. Electron microscopy (FE-SEM) studies showed that the surface of
43 cellulose after mechanochemical treatment was rough with no presence of fibres.

44

45
46 Abbreviations: DMAc: N,N-dimethylacetamide; FE-SEM: field emission
47 scanning electron microscope; ICP-MS: inductively coupled plasma mass
48 spectroscopy; RSD: relative standard deviation; SD: standard deviation; SWDP:
49 softwood dissolving pulp; WAXD: wide angle X-ray diffraction

50 Introduction

51 Cellulose is an abundant natural polymer suitable for making a large variety of materials and
52 chemicals. Several cellulosic derivatives can be compounded, pelletized and processed, depending
53 on the cellulose derivative and compounding conditions. Some of the classical tools for
54 thermoplastic processing are extrusion, injection or blow moulding, spinning and film forming
55 (Quintana et al. 1995).

56 However, the use of these techniques for processing pure cellulose is impossible since the
57 polymorphs of cellulose I and II does not melt. Recently, several attempts were made to shape
58 pure cellulose, mainly wood pulp, without any chemical treatment. One such study is the
59 compression moulding of wood fibre materials. Researchers used only water as a processing aid
60 and at the end they obtained all-cellulose composite plaques from pulp of high cellulose purity
61 (Nilsson et al. 2010). In another study, cellulose was plasticized, without chemical modification,
62 by the use of the combination of mechanical shear, uniaxial pressure and laser radiation (Schroeter
63 and Felix 2005).

64 Since cellulose does not melt, processing of cellulose materials is usually based on dissolution in
65 solvents and regeneration to two-dimensional objects such as fibres and films. However, cellulose
66 among other features has a complex system of hydrogen bonds that prohibits dissolution of
67 cellulose in common organic and inorganic media. Disruption of hydrogen bond network can be
68 done mechanically or chemically. Cellulose with complete amorphous structure is usually
69 prepared by ball milling (Zhang et al. 2007). Another alternative to interrupt this hydrogen
70 bonding network is by using high pressure treatments. When polymers are subjected to high
71 pressure, a rearrangement at all levels of their structural organization occurs (Ioelovich 2008).
72 Structural rearrangements in polymers subjected to high pressure may be related to possible
73 changes in the intensity of intermolecular interactions. In the case of cellulose, X-ray diffraction
74 analysis suggests that the crystalline phase may be destroyed, leaving an amorphous state (Zhorin
75 et al. 2010). Beside the mechanical methods, there are several chemical treatments for producing
76 amorphous cellulose. Reported methods are deacetylation of cellulose acetate under non-aqueous
77 alkaline conditions (Wadehra and Manley 1965) and regeneration of cellulose dissolved in
78 different solvent systems (Ciolacu et al. 2011; Volkert and Wagenknecht 2008). The disadvantage
79 with conventional amorphous cellulose is its tendency to recrystallize into cellulose II in the
80 presence of water.

81 Physical and chemical properties of cellulose are strongly influenced by the arrangement of the
82 cellulose molecules. There are two types of hydrogen bonds present in cellulose fibres viz.,
83 intramolecular interactions occurring between the C-3 OH group and oxygen of the pyranose ring,
84 and intermolecular hydrogen bonds occurring between the C-6 OH group and oxygen of the
85 glucosidic bond of another molecule. Hydrogen bonds form cellulose crystallites that are very
86 difficult to penetrate by solvent molecules. Furthermore, if the starting material is amorphous
87 cellulose, reactivity of chains will be much higher, for example, the enzymatic hydrolysis of
88 cellulose to glucose (Haan et al. 2007). Besides its high reactivity, amorphous cellulose is
89 necessary for drawing and shaping process. Togawa and Kondo (1999) investigated the drawing
90 process of cellulose films. In order to achieve high draw ratio, hydrogen bonds needed to be
91 dissociated during the drawing process. The drawability is hindered by intermolecular hydrogen
92 bonds, since these bonds restrict the mobility of polymer chains. For successful drawing of
93 cellulose films, hydrogen bonds were suppressed prior to the drawing process, with DMAc/LiCl
94 solvent system. Processing of natural materials such as wood or cellulose is not as convenient as
95 processing synthetic polymers. Conventional processing of synthetic polymers involves thermal
96 processing. Higher temperatures in thermal process of natural materials lead to the decomposition
97 of materials before melting. Zhang (2012) presented a process for producing plastic cellulose
98 material without chemical modification or addition of additives. Cellulose powder was ball milled
99 before it was subjected to the back pressure equal channel angular pressure. The purpose of this
100 mechanical pretreatment was to disrupt the cellulose particles and enhance the chain entanglement.
101 The storage modulus was higher for the ball-milled samples compared to the un-milled ones. The

102 XRD results showed the decrease in crystallinity and crystal size. Crystallinity of cellulose powder
103 was reduced, which allowed production of cellulose plastics under the strong shear-deformation
104 conditions.
105 Swelling process of cellulose fibres prior to dissolution is an important step of cellulose chemistry
106 and technology. Main part in the interactions of cellulose with external agent is the change in
107 morphology. The swelling of cellulose in various solvent systems has been the subject of
108 numerous investigations. The heterogeneous swelling of the fibres was observed long time ago in
109 chemical mixtures like sodium hydroxide or N-methylmorpholine N-oxide (NMMO) in water. The
110 same mechanisms were also observed when using solvents like ionic liquids (Cuissinat et al.
111 2008a) and other chemicals (Cuissinat 2006). From all these studies, it was shown that the key
112 parameter in the dissolution mechanism is the morphology of the fibre. If the original wall
113 structure of the native fibre is preserved, the dissolution mechanisms are mostly similar to wood,
114 cotton, and other.
115 The present research work aims to take advantage of the modifications in the intermolecular
116 interactions, wherein a swelling treatment enables cellulose moulding. Cellulose pulp was thus
117 swollen with DMAc/LiCl solvent system, washed and dried before further processing. Formability
118 of these treated cellulose samples were evaluated. The objective of this study was to explore the
119 possibilities of moulding pre-swollen cellulose materials and to understand the role of disrupting
120 the intermolecular bonds of cellulose without derivatization.

121 **Materials and Methods**

122 *Materials*

123 Softwood dissolving pulp was acquired from Domsjö Fabriker, Sweden. Dissolving pulp is
124 produced from a controlled mixture of spruce and pine (60%:40%) by a two-stage sodium based
125 cooking to give a sulphite pulp with very low lignin content (0.6%) and high alpha- cellulose
126 content (93%). The viscosity of pulp was 530 ± 30 ml/g according to ISO 5351 standard and the
127 degree of polymerization was 780 (Domsjö 2011). Cellulose was swollen with *N,N*-
128 dimethylacetamide (Sigma-Aldrich, Finland) and lithium chloride (Merck, Finland). Acetone was
129 purchased from J.T. Barker. All chemicals were used as received without further purification.
130

131 *Swelling of pulp in DMAc/LiCl solvent system*

132 The pulp was first chopped into small pieces of 2.0 g each. Swelling of softwood dissolving pulp
133 in DMAc/LiCl involves the following solvent exchange procedure. Initially, each cellulose sample
134 was suspended in 300 cm³ distilled water for 1h at room temperature. After filtration, it was
135 immersed into 200 cm³ acetone for 1h and subsequently, into 100 cm³ *N,N*-dimethylacetamide for
136 1h at room temperature. 50 cm³ DMAc was heated to 40 °C followed by the addition of 3.0 g
137 Lithium chloride to the solution. When the swelling procedure was finished, a transparent gel was
138 formed. The gel was solidified by distilled water and exchanged for fresh distilled water after 1h,
139 4h and 12h. After solidification, the cellulose referred hereafter as Cell_DL was dried at room
140 temperature for further processing. Second solidification procedure involves the washing of
141 transparent gel with solvent composed of isopropyl alcohol and deionized water (40:60). Samples
142 were washed twice with 100 ml of this solvent. After washing, the samples were soaked in 300 ml
143 deionized water to remove residual isopropyl alcohol. Further to remove Lithium from cellulose,
144 samples were exposed to running tap water overnight (Nayak et al. 2008) and the resultant product
145 will be referred hereafter as Cell_RS. The whole experimental part is depicted in Figure 1.

146
147 ((Figure 1))

148 *Moulding of swollen cellulose specimens*

149 A cylindrical mould (Fig. 2) with a piston was built in stainless steel. Dried sample was put in the
150 mould, closed with the piston and placed on a regular hydraulic press (Enerpac bench press).
151 Sample was pressed at about 70 MPa vertical pressure for a couple of seconds at room temperature
152 (Fig. 3)
153

154 ((Figure 2))
155 ((Figure 3))

156
157
158

159 *Optical microscopy*

160
161
162
163
164
165

Swelling mechanism of cellulose in DMAc/LiCl solvent system was studied with a Nikon Eclipse E200 optic microscope attached to a Nikon DS-Fi2 digital camera. Swelling treatment was recorded after 10 minutes, 20 minutes and 30 minutes.

166 *Determination of crystallinity using X-ray diffraction (XRD)*

167 X-ray diffraction measurements were performed on a goniometer (PW3020) using CuK α radiation
168 generated at 30 mA and 40 kV. The CuK α radiation consists of K α 1 (1.54060 nm) and K α 2
169 (1.54443 nm) components. Dried cellulose samples were cut and put on plastic substrate. Scans
170 were obtained from 15 to 70°, 2 θ degrees in 0.02 degree steps for 1.5 seconds per step. Degree of
171 crystallinity (I_c) was calculated from the ratio of the height of 002 peak (I_{max}) and the height of the
172 minimum between the 002 and 101 peaks, shown in equation (1):

$$173 \quad I_c = 1 - \frac{I_{min}}{I_{max}} \quad (1)$$

174 *Determination of cellulose structure using Raman spectroscopy (FT-* 175 *Raman)*

176 Cellulose samples were analysed with The Thermo Scientific Nicolet iS50 spectrometer. The
177 Raman system is equipped with 1064 nm diode laser. The laser power used for chemically treated
178 sample excitation was 500 mW, and 1024 scans were accumulated. Reference pulp was excited
179 with 0.35 W power, and 32 scans were collected. Omnic software program was used to find peak
180 positions and process the spectral data.

181 *Determination of Lithium ion concentration analysed by ICP-MS*

182 The samples are first digested with a microwave digestion system from Anton Paar, Multiwave
183 3000. Sample amount have been balanced in a range of 0.1 g to which have been added 5 cm³ 65%
184 HNO₃ suprapur from Merck and 1 cm³ 30% H₂O₂ suprapur. The temperature in the microwave
185 oven was up to 200 °C. The analysis was performed with a ICP-MS from PerkinElmer Sciex Elan
186 6100 DRC+. The standardization has been done with a multi standard from ULTRA SCIENTIFIC,
187 item: IMS-102. The analyzing method has been the standard performance with the following
188 parameters: Sweeps: 11; Replicates: 7; Dwell time: 100; 10 ppb Rh was used as an internal
189 standard solution.

190 *Field Emission Scanning Electron Microscope (FE-SEM)*

191 The morphology of samples was examined by a Leo Gemini 1530 field emission scanning electron
192 microscope with In-Lens detector. After moulding, samples were dried in air and sectioned using a
193 doctor blade prior to be coated with carbon in Temcarb TB500 sputter cater (Emscope
194 Laboratories, Ashford, UK). Optimum accelerating voltage was 2.70 kV and magnifications were
195 1,500; 10,000; 25,000 and 50,000X.

197 *Mechanical characterization*

198

199 Mechanical properties of cellulose samples were measured with UBI1 Nanomechanical Test
200 Instrument (HYSITRON, Inc.) using a continuous stiffness measurement in a force controlled
201 mode with Berkovich type triangular diamond pyramid. Continuous stiffness measurement
202 technique offers measurements of contact stiffness, hardness, elastic modulus, creep resistance,
203 and fatigue properties of materials. Nanoindentation elastic modulus (E) and hardness (H) are
204 defined with following equations (2) and (3):

$$205 \quad E = \frac{dP}{dh} \frac{1}{2} \sqrt{\frac{\pi}{A}} \quad (2)$$

206

$$207 \quad H = \frac{P_{max}}{A} \quad (3)$$

208

209 Where P_{max} is the applied load at the maximum depth of penetration, A is the contact area and $\frac{dP}{dh}$
210 is the slope of the initial portion of the unload curve in the load-displacement plot. Prior to
211 Nanoindentation tests, cellulose samples were pressed with Pellet Press of FTIR. At least 6
212 indentations were performed on each sample, with the peak load force of 5000 μN for sample
213 where solvent was removed with 2-propanol and deionized water and 200 μN for swollen sample
214 washed with just distilled water.

215

216

217 **Results**

218 *Swelling of cellulose in DMAc/LiCl solvent system*

219 Swelling of cellulose fibers in DMAc/LiCl solvent system is also a heterogeneous process. When
220 fibers are placed in DMAc/LiCl, solvent molecules penetrate only to the semi-permeable and
221 elastic parts of the fiber wall. The diffused molecules cause radial expansion of the secondary wall.
222 These localized swollen parts along the fiber gives the impression of balloons (Navard and
223 Cussinat 2006). The balloons were formed in the first couple of minutes. In the course of swelling,
224 balloons were bursting and fragments arise. After 30 minutes of treatment, a two phase system was
225 visible. It can be observed from Figure 4, that there were some intact fibers still exist. In the
226 swelling process Cl^- ions formed hydrogen-type interactions with hydroxyl group hydrogens of
227 cellulose, breaking the existing bonds in the interior of the structure. Meanwhile Li^+ ions
228 interacted with carbonyl group oxygen of DMAc molecule forming $[\text{DMAc}_n + \text{Li}]^+$ macrocations.
229 Macrocations acted as a spacer between cellulose chains prohibiting the formation of
230 intermolecular hydrogen bonds. When fibers swell, intermolecular bonds are broken as a result of
231 the stress produced by swelling process. With a very strong solvent it is possible to disrupt the
232 entire crystalline structure (Mantanis et al. 1995). In this particular case swelling of 30 minutes
233 was sufficient to reduce crystallinity of fibers to the necessary amount with which molding process
234 is possible. Shorter swelling time would not decrease the crystallinity sufficiently, and this results
235 in a brittle non-mouldable material. Longer swelling time would go to dissolution stage, where
236 cellulose II would arise.

237

238

239 ((Figure 4))

240

241 *Effect of swelling treatment on crystallinity analysed by XRD*

242 Native and most regenerated cellulose consists of crystalline and non-crystalline domains. The
243 physical properties and reactivity of cellulose is strongly influenced by the arrangement of
244 cellulose molecules. Interactions between cellulose and reactive substances occur first in non-
245 crystalline domains. The X-ray patterns of reference pulp, sample washed with distilled water

246 (Cell_DL) and sample washed with organic solvent (Cell_RS) are presented in Figure 5. X-ray
247 diffractogram for the reference softwood dissolving pulp had two peaks, characteristic of the
248 cellulose I crystal structure. The crystalline structure of softwood pulp was lost after swelling in
249 DMAc/LiCl and solidifying with distilled water. Duchemin (2007) studied the transformation of
250 microcrystalline cellulose due to partial dissolution in 8% DMAc/LiCl. His work helped in
251 understanding the phase transformation that occurs during dissolution in this particular solvent
252 system. Dissolution occurs through the continuous peeling of layers of crystal domains. The
253 peeled layers may retain some cellulose I structure from which they were removed, but generally
254 they were too thin to contain crystallite chains. This is the reason that precipitated peeled layers
255 seemed as amorphous cellulose. Significant crystalline diffraction was not observed in Cell_DL
256 specimens, indicating that the slow solidification of samples in distilled water produced crystallites
257 of a small size or with imperfections in the crystalline structure. Cell_RS specimen has diffraction
258 peaks at 15.0° and 22.3° , indicating cellulose I structure. Although the sample had same
259 crystallinity pattern as native cellulose, swelling treatment resulted in a decrease in the degree of
260 crystallinity from 0.54 to 0.43.

261
262 ((Figure 5))

263 264 *Effect of swelling treatment on cellulose structure analysed by FT-Raman*

265
266 Raman spectra in the frequency region $300-3700\text{ cm}^{-1}$ for the reference pulp, Cell_DL and
267 Cell_RS are shown in Fig. 6, which infers the spectral changes occurred upon the loss of
268 crystallinity. Between 1000 and 1200 cm^{-1} , there are ring bond stretches and C–O stretches. The
269 angle bends (CCC, OCC, COC, OCO), C–O stretches, and methylene bending appear between 700
270 and 800 cm^{-1} . Between 400 and 600 cm^{-1} are the heavy atom bending, C–O and ring bending, and
271 some ring stretching. And between 200 and 400 cm^{-1} are ring torsions. Spectrum of a crystalline
272 substance contains sharp discrete bands whereas the amorphous materials contain broad diffuse
273 bands (Socrates 2001). The broad band in the $3100-3600\text{ cm}^{-1}$ region that was due to the OH-
274 stretching vibrations gave information concerning the hydrogen bonds. The peak characteristic of
275 hydrogen bonds from the Cell_DL sample became wider in comparison to the peak from reference
276 pulp, which can be correlated with the interruption of the intra- and intermolecular hydrogen bond
277 by swelling treatment. The Cell_DL spectrum exhibits a strong band at 605 cm^{-1} which is due to
278 the bending motion of the O=C–N group of DMAc molecule. Amide I band characteristic for C=O
279 stretching vibration can be seen at 1650 cm^{-1} . This band is a typical carbonyl adsorption band of
280 tertiary amides. The Raman spectrum from sample Cell_RS was similar to reference pulp, except
281 for the missing 605 cm^{-1} and 1650 cm^{-1} peaks. In general, all amides have one or more bands of
282 medium-to-strong intensity, which may be broad, in the region $695-550\text{ cm}^{-1}$ which are probably
283 due to the bending motion of the O=C–N group. The carbonyl absorption band of tertiary amides
284 occurs in the region $1670-1630\text{ cm}^{-1}$. The lack of these two peaks indicates the absence of DMAc
285 in Cell_RS samples.

286
287 ((Figure 6))

288 289 *Residual of Lithium analysed by ICP-MS*

290 Concentration of Li ions in cellulose samples was measured with inductively coupled plasma mass
291 spectroscopy as a function of treatment time in the solvent. As shown in the Table 1, Li⁺ ion
292 concentration revealed that, cellulose samples after swelling with DMAc/LiCl contained more
293 lithium ion than compared with the reference soft dissolving pulp. The small size of Li⁺ ions
294 allows them to interact with glucan chains, including more restricted regions near the oxygen
295 linkers. The concentration of Li⁺ ions decreased from 672.04 to 526.98 ppm with decrease in the
296 swelling time from 30 to 20 minutes. It can be concluded that Li⁺ ions stayed between cellulose
297 chains, and the amount of Li⁺ ions is affected by the swelling time. Specimens solidified with 2-
298 propanol and deionized water had significantly lower amount of Lithium ions, indicating that
299 solvent removed most of the cations. Taking into account the result from Raman spectroscopy of
300 specimen Cell_RS, it can be concluded that most of the DMAc/LiCl is expelled. This is in
301 agreement with findings of Nayak and co-workers (2008). Their study showed insignificant
302 amount of DMAc and Li⁺ ions (10.61 ppm) present in the films even after washing with a 2-
303 propanol and deionized water mixture, and subjecting it to running water. Observed difference
304 between Cell_DL and Cell_RS samples regarding the content of retained Lithium cation might be

305 due to the final exposure to water. Time Cell_DL samples spent in a beaker with distilled water
306 was in total 29 hours, while Cell_RS samples were exposed to running water over night. Even
307 before the exposure to water, Cell_RS sample had a lower amount of macrocation. Majority of
308 macrocation was already washed with anti-solvent composed of 2-propanol and deionized water.
309 This solvent has a lot more power in dissociating cellulose with solvent complex.

310 *Effects of swelling treatment on the morphology of fibres analysed by FE-* 311 *SEM*

312 The morphological structure of cellulose samples treated with DMAc/LiCl and moulded was
313 observed using scanning electron microscopy. The scanning electron micrographs (Fig. 7) showed
314 the heterogeneous and rough surface of cellulose moulded samples. This is consistent with the
315 findings of Yun and co-workers (2008). In their study, curing of cellulose previously dissolved in
316 DMAc/LiCl with deionised water led to objects with wrinkled rough surface and non-
317 homogeneously generated layered structure. FE-SEM images (Fig. 8) demonstrate the microfibril
318 bundles structure. Similar discovery was reported by Wei and Cheng (2007) when they studied the
319 effect of solvent exchange on the structure of cellulose. They concluded that solvent activation
320 prior to dissolution of cellulose led to the fibrillation of treated fibre surface. These findings
321 indicated that chemical and mechanical treatment of cellulose caused destruction of cell wall
322 organisation and led to re-organisation of microfibrils into layers. Fibrils are destroyed by swelling
323 treatment, and reassembled in a whole new structure. SEM images of Cell_RS samples were not
324 taken, since moulding step wasn't possible to perform.

325
326 ((Figure 7))

327 ((Figure 8))

328

329 *Mechanical Properties*

330

331 The nanoindentation tests were used to investigate mechanical properties of cellulose sample. The
332 elastic modulus and hardness of specimens measured by nanoindentation are shown in Table 2.
333 The surface roughness had impact on the measurement especially for the shallow penetrations, so
334 average values were calculated from 18th till 33rd cycle. Both hardness and elastic modulus were
335 significantly higher in Cell_RS compared to that of Cell_DL. Results of mechanical testing for
336 Cell_DL samples were expected since specimens had amorphous structure, which made them less
337 rigid, weaker and easily deformed. Solvent trapped in samples affects the surface morphology and
338 mechanical properties of the material. Trapped [DMAc_n+Li]⁺ macrocations hinder cellulose to
339 form ordered structure by weakening the inter-molecular hydrogen bonds between cellulose chains
340 which results in low mechanical properties (Yun et al. 2008). Cellulose samples with crystalline
341 structure have higher hardness and elastic modulus. Increased crystallinity is associated with
342 increase in rigidity and hardness. Our results suggest that disruption of hydrogen bonding network
343 via intermolecular non-covalent bonding allows the preparation of mouldable cellulose.

344

345 **Conclusions**

346 The objective of this study was to prepare moldable cellulose materials without chemical
347 modification. Cellulose swelling is essential for producing cellulose products. DMAc/LiCl solvent
348 system was used to swell cellulose with the aim to broaden its application in producing functional
349 materials. Swelling process was necessary in breaking the existing bonds in the interior of the
350 structure, thus lowering crystallinity of cellulose fibers. Reduced crystallinity can be even more
351 diminished by preserving solvent between cellulose chains. It can be accomplished using distilled
352 water as an anti-solvent. Retained swelling solvent acted as a spacer between cellulose chains
353 prohibiting formation of intermolecular hydrogen bonds. Separated cellulose chains had disordered
354 structure, which made them ductile and easily deformed. If solvent is washed away from
355 specimens with mixture of isopropyl alcohol and deionized water, intermolecular hydrogen bonds
356 are reformed. In that case material became brittle and lost its feasibility for molding. Three
357 dimensional cellulose objects can be produced only if the DMAc/LiCl solvent system is present in

358 cellulose specimens. Our future research will focus on alternatives to mimic this behavior using
359 solvents/agents which are easier to recycle and upscale to industrial applications.

360 **Acknowledgments** This work is part of Future Biorefinery (FuBio) project, funded by TEKES and
361 coordinated by Finnish Bioeconomy Cluster (FIBIC).

362

363 References

364

365 Ciolacu D, Ciolacu F, Popa IV (2011) Amorphous cellulose-structure and characterization.
366 Cellulose Chem Technol 45:13-21

367

368 Cuissinat C (2006) Swelling and dissolution mechanisms of native cellulose fibres. PhD
369 dissertation, Ecole Nationale Supérieure des Mines de Paris, Sophia-Antipolis, France

370

371 Cuissinat C, Navard P, Heinze, T (2008a) Swelling and dissolution of cellulose, Part IV: Free
372 floating cotton and wood fibres in ionic liquids. Carbohydr Polym 72:590–596

373

374 Domsjö (2011) Specification Domsjö cellulose. <http://www.domsjoe.com>. Accessed 01 Feb 2012

375

376 Duchemin BZ, Newman HR, Staiger PM (2007) Phase transformation in microcrystalline
377 cellulose due to partial dissolution. Cellulose 14:311-320. doi: 10.1007/s10570-007-9121-4

378

379 Haan DR, Rose SH, Lynd LR, van Zyl WH (2006) Hydrolysis and fermentation of amorphous
380 cellulose by recombinant *Saccharomyces Cerevisiae*. Metab Eng 1:87-94

381

382 Ioelovich M (2008) Cellulose as a nanostructured polymer: a short review. Bioresour 3:1403-1418

383

384 Mantanis GI, Young RA, Rowell RM (1995) Swelling of compressed cellulose fiber webs in
385 organic liquids. Cellulose 2: 1-22

386

387 Navard P, Cuissinat C (2006). Cellulose swelling and dissolution as a tool to study the fiber
388 structure. 7th International Symposium 'Alternative Cellulose: Manufacturing, Forming,
389 Properties'. Rudolstadt, Germany

390

391 Nayak NJ, Chen Y, Kim J (2008). Removal of impurities from cellulose films after their
392 regeneration from cellulose dissolved in DMAc/LiCl solvent system. Eng Chem Res 47:1702-
393 1706

394

395 Nilsson H, Galland S, Larsson TP, Gamstedt KE, Nishino T, Berglund AL, Iversen T (2010) A
396 non-solvent approach for high-stiffness all-cellulose biocomposites based on pure wood cellulose.
397 Compos Sci Technol 70:1704-1712. doi:10.1016/j.compscitech.2010.06.016

398

399 Quintana R, Persenaire O, Bonnaud L, Dubois P (2012) Recent advances in (reactive) melt
400 processing of cellulose acetate and related biodegradable bio-compositions. Polym Chem 3:591-
401 595. doi: 10.1039/C1PY00421B

402

403 Schroeter J, Felix F (2005) Melting cellulose. Cellulose 12:159-165. doi: 10.1007/s10570-004-
404 0344-3

405

406 Socrates G (2001) Infrared and Raman characteristic group frequencies, 3rd edn, John Wiley and
407 Sons Ltd, West Sussex

408

409 Togawa E, Kondo T (1999) Change of morphological properties in drawing water-swollen
410 cellulose films from organic solutions. A view of molecular orientation in the drawing process. J
411 Polym Sci 37:451-459

412

413 Volkert B, Wagenknecht W (2008). Substitution patterns of cellulose ethers- Influence of the
414 synthetic pathway. Macromol Symp 262:97-118

415

416 Wadehra IL, Manley J (1965) Recrystallization of amorphous cellulose. *J Appl Polym Sci* 9:2627-
417 2630
418
419 Wei Y, Cheng F (2007) Effect of solvent exchange on the structure and rheological properties of
420 cellulose in LiCl/DMAc. *J Appl Polym Sci* 106:3624-3630. doi:10.1002/app.26886
421
422 Yun S, Chen Y, Nayak NJ, Kim J (2008) Effect of solvent mixture on properties and performance
423 of electro-active paper made with regenerated cellulose. *Sens Actuators B: Chem* 129:652-658.
424 doi:10.1016/j.snb.2007.09.049
425
426 Zhang W, Liang M, Lu C (2007) Morphological and structural development of hardwood cellulose
427 during mechanochemical pretreatment in solid state through pan-milling. *Cellulose* 14:447-456.
428 doi: 10.1007/s10570-9135-y
429
430 Zhang X, Wu X, Gao D, Xia K (2012) Bulk cellulose plastic materials from processing cellulose
431 powder using bulk pressure-equal channel angular pressing. *Carbohydr Polym* 87:2470-2476
432
433 Zhorin AV, Kiselev RM, Zelenetskii NA, Rudakova AT (2010) Calorimetric investigation of some
434 polysaccharides subjected to high-pressure plastic deformation. *Polym Sci* 52:398-406.
435 doi:10.1134/s0565545x10040085

436 **Table 1** Determination of lithium ion concentration with ICP-MS for reference pulp, cellulose
437 containing DMAc/LiCl (Cell_DL) and cellulose where DMAc/LiCl was removed (Cell_RS).
438

Sample	Content mg/kg	SD mg/kg	RSD %
Reference	0.02	0.01	64.90
Cell_DL, 30 min	672.04	17.80	2.60
Cell_DL, 20 min	526.98	8.73	1.20
Cell_RS, 30 min	1.79	0.02	1.30

439

440 **Table 2** Mechanical properties measured with nanoindentation for cellulose containing
441 DMAc/LiCl (Cell_DL) and cellulose where DMAc/LiCl was removed (Cell_RS).
442

Sample	Elastic modulus, MPa	Hardness, MPa	Force, μN	Depth, nm	Cycle
Cell_DL	54	6.5	200	3932	33
Cell_RS	6993	381.4	5000	2839	33

443
444

445
446
447
448
449
450
451
452
453
454
455
456
457
458
459
460
461
462
463
464
465
466
467
468
469
470
471
472

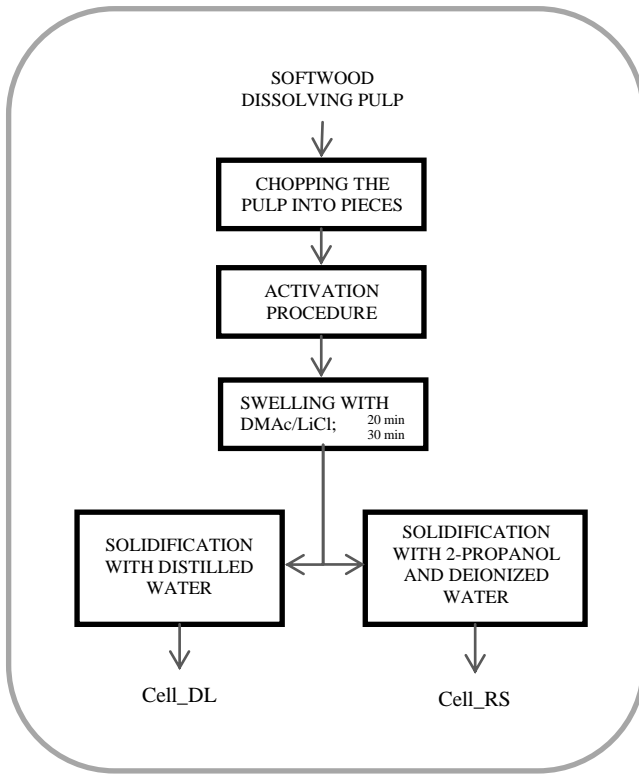
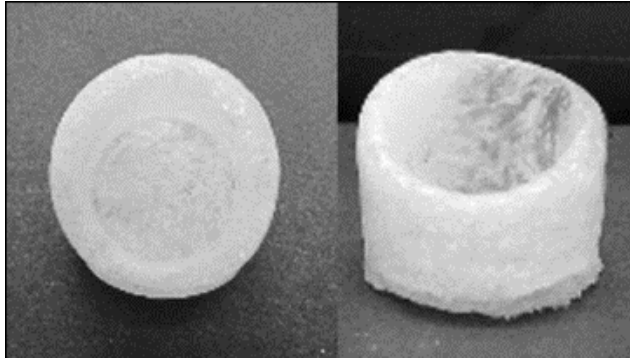


Fig. 1 Schematic representation of the experimental work.



473
474
475

Fig. 2 Pictures of prototype mould from stainless steel



476
477
478
479

Fig. 3 Images of the moulded sample (Cell_DL)

480
481
482
483
484
485
486
487
488

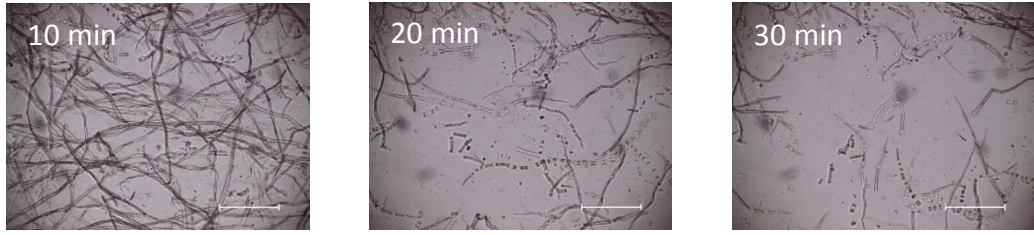
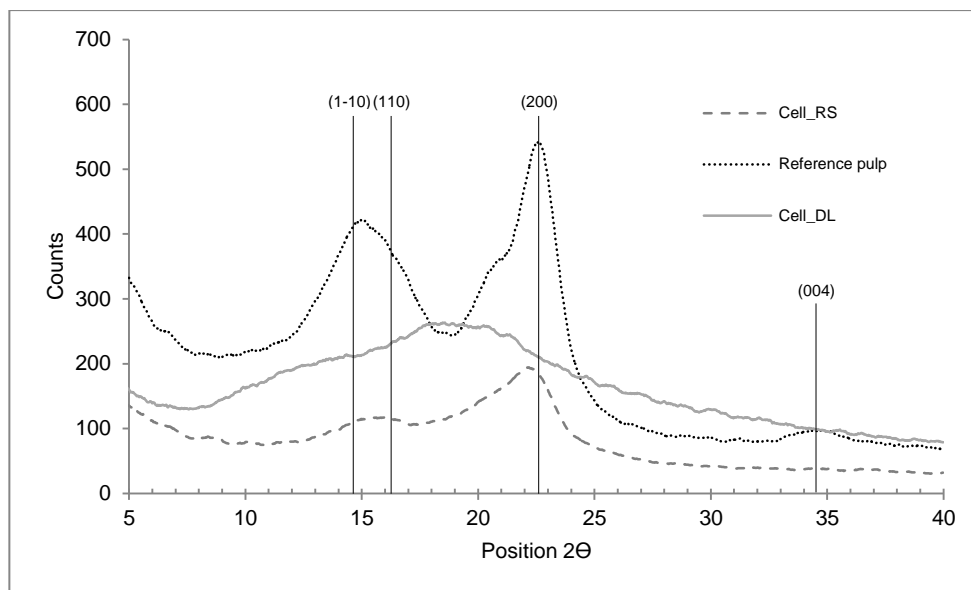
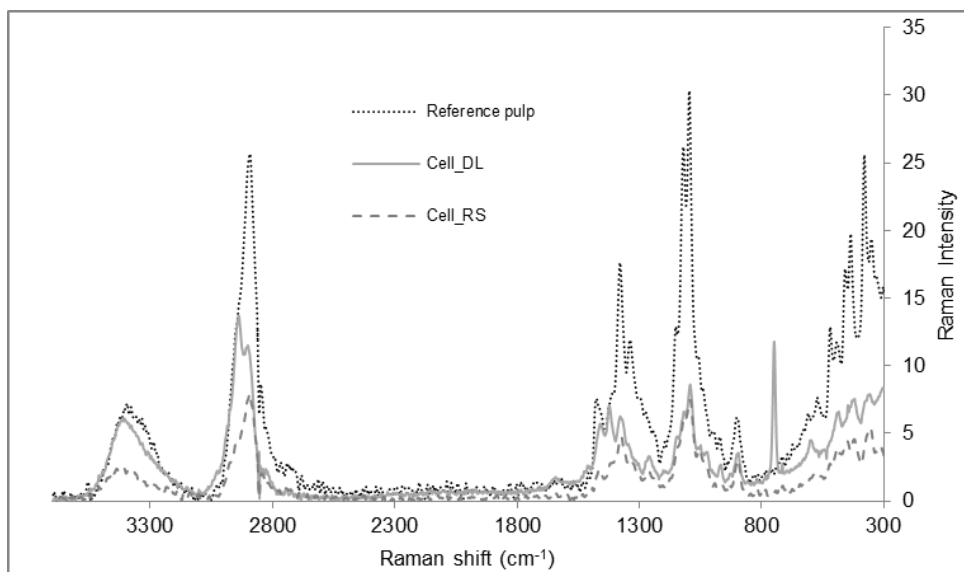


Fig. 4 Optical micrographs during the swelling process of cellulose in DMAC/LiCl solvent sytem.
Bar represents 500 μm .



489
 490
 491
 492
 493

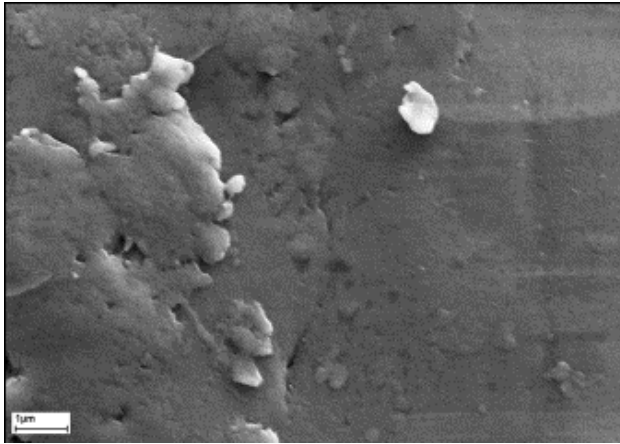
Fig. 5 X-ray diffractogram of reference pulp, swollen cellulose washed with distilled water (Cell_DL) and swollen cellulose washed with mixture of 2-propanol and deionized water (Cell_RS)



494
495
496
497

Fig. 6 Raman spectra for reference pulp, swollen cellulose washed with distilled water (Cell_DL) and swollen cellulose washed with mixture of 2-propanol and deionized water (Cell_RS)

498

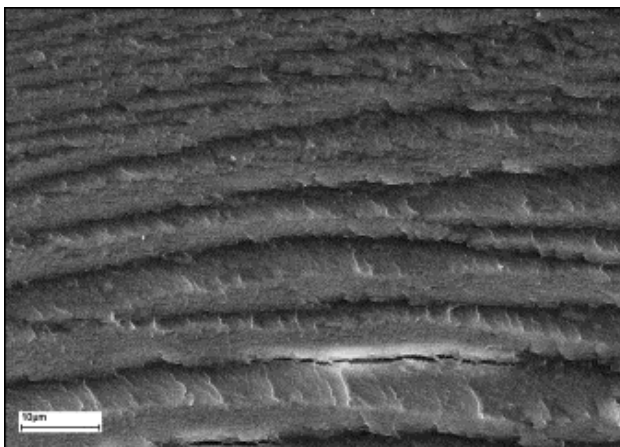


499

500

501

(a)



502

503

504

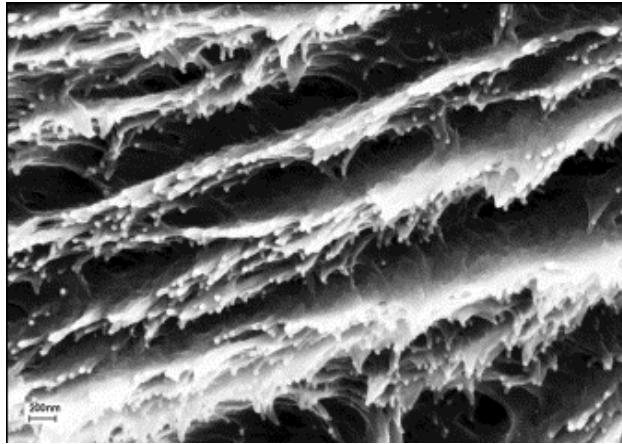
505

506

(b)

Fig. 7 SEM images of the swollen cellulose surface Cell_DL (magnification (a) 10,000 x and (b) 1,500 x)

507

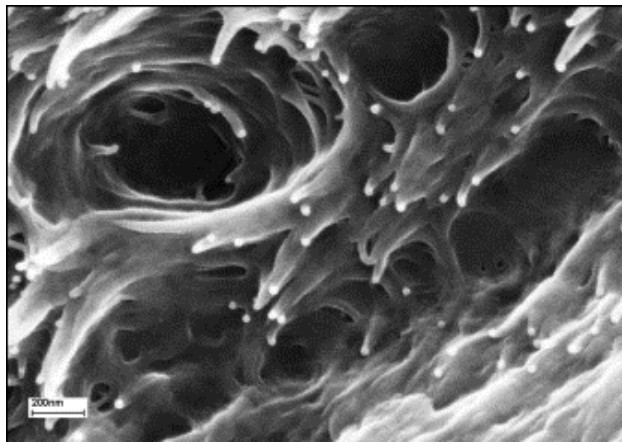


508

509

510

(a)



511

512

513

514

515

516

(b)

Fig. 8 SEM cross-sectional images of the swollen cellulose Cell_DL (magnification (a) 25,000 x and (b) 50,000 x)